ELSEVIER

Journal of Structural Geology 27 (2005) 1892–1898

JOURNAL OF STRUCTURAL GEOLOGY

www.elsevier.com/locate/jsg

Evaluation of asperity-scale temperature effects during seismic slip

Kieran O'Hara*

Department Geological Sciences, University of Kentucky, Lexington, KY 40506, USA

Received 2 February 2004; received in revised form 20 January 2005; accepted 20 April 2005
Available online 11 August 2005

Abstract

For the common rock-forming minerals, the Joule–Thompson effect produces cooling on compression and heating on decompression. Experimental rock friction studies and seismological evidence suggest that the strength of faults is controlled by high-stress asperities that represent a small fraction of the total fault area. During seismic rupture, the area immediately beneath asperities is inferred to undergo adiabatic compressions and decompressions on the order of 1–2.8 GPa. Joule–Thompson coefficients are in the range 261–372 °C/GPa, resulting in temperature changes of ±336–880 °C. Quartz asperities with a compressive strength of 2.8 GPa can produce a heating or cooling of 880 °C immediately beneath an asperity. By comparison, frictional heating 'flash temperatures' are less than 1000 °C for asperity contact areas $<300\ \mu m^2$. The Joule–Thompson effect is independent of asperity size and may augment or counteract frictional heating. The paucity of pseudotachylytes in the geologic record and the absence of localized heat flow anomalies on active faults might be explained by the Joule–Thompson cooling effect.

Keywords: Adiabatic; Decompression; Friction; Pseudotachylyte; Earthquake

1. Introduction

Pseudotachylytes are commonly thought to be solely the product of frictional heat during seismic slip (Sibson, 1975). Macroscopically, the rate of heat generation per unit fault area (Q) is normally taken as the product of the shear stress (τ) times the velocity of slip (v):

$$Q = v\tau \tag{1}$$

On a microscopic scale, however, faulting involves the interaction of asperities whose area of contact is a small fraction of the total fault area. This may lead to locally very high stresses. In addition, locally very high temperatures are possible due to frictional heating on asperities (so called 'flash temperatures'; Archard, 1958–59). The interaction, failure, and time dependent healing behavior of the asperities may control seismic behavior, frictional heat, wear volume and rupture strength of faults (Scholz, 2002). Understanding the microscopic behavior of asperities is therefore important for understanding rock friction in general (Logan and Teufel, 1986; Dieterich and Kilgore, 1994, 1996) and more specifically, the dissipation of work as heat during seismic slip (O'Hara, 2001).

During high strain rate events there are rapid compressions and decompressions associated with deformation. For example, adiabatic decompression is widely thought to produce melting during meteorite impact (Melosh, 1989). Waldbaum (1971) explored the heating effect of adiabatic decompression on rapidly ascending magmas. More recently, Bjornerud and Magloughlin (2004) suggested that dilatational faulting at depth in the crust may lead to decompressional melting. Seismic (Nadeau and Johnson, 1998), experimental (Logan and Teufel, 1986), and theoretical studies (Sammis et al., 1999) suggest that asperities may be very strong so that stress drops during earthquakes may be locally very large. Fault-related pseudotachylytes invariably show a large concentration of lithoclasts embedded in the melt, and this texture is usually interpreted as mechanical wear production due to shearing off of asperities, followed by frictional melting (Spray, 1995). Together these observations suggest that, during seismic slip, there may be large rapid compressions and decompressions associated with asperity behavior.

It is shown here that adiabatic compression and

* Fax: +1 606 323 1938.
E-mail address: geokoh@uky.edu.

0191-8141/$ - see front matter © 2005 Elsevier Ltd. All rights reserved.
doi:10.1016/j.jsg.2005.04.013

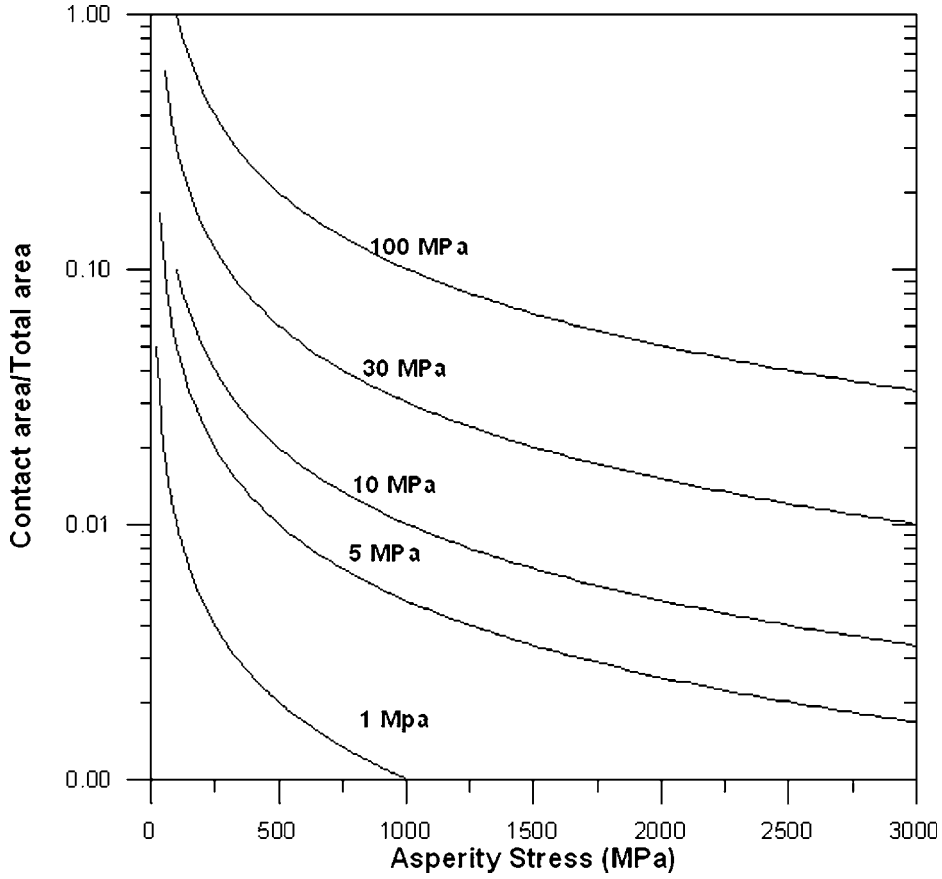

Fig. 1. Plot of asperity stress versus real area of contact/total area for different average fault normal stresses. For a given average normal stress, the asperity stress is strongly magnified at lower real contact areas.

decompression beneath an asperity can result in several hundred degrees heating or cooling, which, provided the asperities are small enough, is of the same order of magnitude as frictional heating. The results suggest that Joule–Thompson adiabatic heating and cooling may play an important role in the temperature evolution of a fault during seismic slip.

2. Asperity behavior during seismic faulting

During brittle faulting it is commonly assumed that frictional processes, such as wear production, frictional heat, seismic behavior, and fault strength, are governed by small areas of contact between the opposing fault surfaces such that these areas (asperities) represent the load-bearing framework of the fault (Rabinowicz, 1995; Sammis et al., 1999; Scholz, 2002). The real area of contact A_r between the fault surfaces is usually only a fraction of the total area A_t, so that if the average normal stress on the fault plane is σ_n, the stress on individual asperities will be magnified by a factor (A_t/A_r). Fig. 1 shows asperity stress versus contact area/total area for a range of average fault normal stresses. For example, a real area of contact (A_r/A_t) of 0.01 and an average fault normal stress of 10 MPa produces an asperity normal stress in excess of 1 GPa. Reducing the contact area to 0.003 results in an asperity stress of approximately 3 GPa. For small earthquakes at Parkfield on the San Andreas fault, stress drops of 1–2 GPa are typical and interpreted to represent failure of very strong asperities (Nadeau and Johnson, 1998; Sammis et al., 1999). The real contact area at Parkfield is estimated to be approximately 0.002 (Nadeau and Johnson, 1998).

Frictional studies on metals and rocks indicate that the real area of contact A_r is proportional to the normal stress σ_n and inversely proportional to the compressive strength (related to the hardness, h) of the asperity (Rabinowicz, 1995; Scholz, 2002)

$$A_r = \sigma_n/h \tag{2}$$

As the normal stress increases, the real area of contact increases by three processes, namely growth of existing contacts, coalescence of contacts and appearance of new contacts (Dieterich and Kilgore, 1996). This relationship appears to hold regardless of whether the asperities deform in an elastic or plastic mode. Experimental rock friction studies also indicate that the maximum stress on the asperities correspond to the maximum compressive strength of the asperity itself (Logan and Teufel, 1986; Scholz, 2002). Uniaxial compressive strengths of several rock types

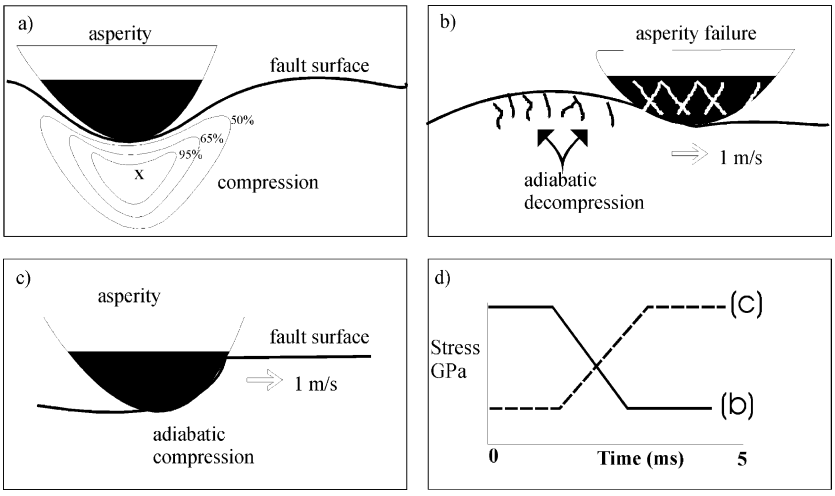

Fig. 2. (a). Schematic diagram showing a strong asperity prior to rupture. The opposing wall is under high stress and elastically deformed. Scale bars omitted. Schematic stress contours are shown as a percentage of the maximum shear stress, based on a steel sphere on an elastically deforming substrate. The maximum shear stress occurs below the surface, suggesting failure may start here (Rabinowicz, 1995, p. 211). (b). After failure initiates, the asperity moves with a velocity of 1 ms^{-1} resulting in adiabatic decompression behind the asperity. The decompression results in heating behind the asperity tip. (c). A strong asperity ploughs a permanent groove (at 1 ms^{-1}) in the opposing wall. The wall undergoes a permanent adiabatic compression, corresponding to the strength of the asperity. The compression results in cooling at the asperity tip. (d). Schematic stress–time diagrams for the asperities described in (b) and (c). The solid line shows the rapid adiabatic decompression immediately behind the failed asperity in (b) and the dashed line shows the adiabatic compression in the case of the asperity in (c). The compressions and decompressions are adiabatic on a millisecond time scale.

are in the range 100–500 MPa at room temperature and moderate confining pressure (Jaeger and Cook, 1979), but the strength of individual minerals is substantially higher (Spray, 1992). Sammis et al. (1999) have argued that if healing of rock or mineral fractures occurs, the asperity strength may approach its theoretical strength (e.g. 1–3 GPa).

During slip, asperities may interact with each other and the opposing fault surface in three different ways (Jaeger and Cook, 1979; Rabinowicz, 1995; Scholz, 2002). An asperity may plough a furrow into the opposing wall, producing wear particles; this is referred to as abrasive wear and is more likely to occur at shallow crustal levels and also if the asperity is harder than the opposing wall. Secondly, asperities may be sheared off and transferred to the opposing wall—this is referred to as adhesive wear and may be more important at deeper crustal levels. Thirdly, asperities may interlock with each other, possibly resulting in either one or both being sheared off, also contributing to the wear volume. Experimental studies (Logan and Teufel, 1986; Dieterich and Kilgore, 1994, 1996) indicate the spatial distribution of asperities is constantly changing, whereby asperities are created and destroyed. The latter workers observed a marked tendency for asperities to cluster, with a power-law size distribution. A clustering of earthquake epicenters was also observed at Parkfield, leading Sammis et al. (1999) to propose a 2-D Cantor dust fractal model for the asperity size distribution.

As an asperity is destroyed (by comminution, shearing or melting), stress may be transferred to an existing asperity, or a new asperity may appear to support the load. More complex asperity behavior is required to explain both time and velocity dependant friction effects (so-called rate/state friction laws), where asperity healing is involved (Dieterich and Kilgore, 1994; summarized in Scholz, 2002). Experimental studies also indicate that wear is characterized by an early transient phase, termed 'running in' of the surface. During the transient stage of wear, the wear rate increases rapidly and then levels off to steady state wear (Power et al., 1988; Rabinowicz, 1995). The latter workers argue, however, that on natural faults the transient wear process remains important even for large displacement because of the self-similar (fractal) nature of the fault surface, which continuously introduces new asperities and roughness (see also Sammis et al., 1999). Other important processes related to the seismic cycle may include chemical reactions that lead to fault weakening or strengthening, or mechanisms such as thermal pressurization, which may be an important weakening mechanism in volatile fault zones. These complex and as yet poorly understood mechanisms are not considered here and the discussion below is confined to mechanical asperity contact models.

3. Stress-time history beneath an asperity

A hemi-spherical asperity with a compressive strength of 2 GPa prior to rupture will stress the opposing wall, which may deform either elastically or plastically. Stress contours for an elastically deforming sphere over an elastically deforming substrate are indicated in Fig. 2a. The maximum shear stress occurs at a shallow depth beneath the surface (x, Fig. 2a), corresponding to the point of maximum yielding (fig. 7.31 in Rabinowicz, 1995). Fig. 2b shows the asperity

Table 1
Joule–Thompson coefficients (μ) and related properties at 400 °C

Mineral	$\alpha_p \times 10^6$ (°C)	V (cm^3)	C_p (J/mol °C)	μ (°C/GPa)	Strength[a] (GPa)	T[b] (°C)
Quartz	69	22.7	69	−314	2.8	±879
Microcline	17	108.7	289	−372	1.6	±595
Plagioclase	12	100.8	296	−338	1.6–2.1	±541–710
Diopside	28	66.1	231	−280	1.2–1.5	±336–420
Olivine	30	46.4	174	−261	2.1–2.8	±548–731

[a] Spray (1992).
[b] Product of μ and strength.

with a velocity of 1 m/s immediately after rupture. As the asperity moves to the right, it may survive for a few additional increments of displacement, so that corresponding compressions and decompression will take place on a short wavelength. However, if it is immediately destroyed (by shearing off, comminution or melting), a decompression is produced in the opposing wall and stress is transferred to a new or existing asperity elsewhere. A measure of the probability that an asperity will be sheared off per unit displacement (the asperity diameter) is given by the wear co-efficient k ($0<k<1$). A value of $k=0.5$ would imply an asperity will be destroyed after two diameter displacements and for $k=0.33$, after three diameter displacements (Scholz, 1987).

An alternative type of asperity behavior is shown in Fig. 2c where a strong asperity ploughs a furrow into a softer opposing wall, producing permanent (non-recoverable) deformation in the opposing wall. In this case, rapid compression is produced immediately beneath the asperity tip during sliding, without a corresponding decompression. Both these types of asperity behavior produce wear particles and belong to the abrasive wear category. Fig. 2d shows schematic stress-time diagrams for both types of behavior. In the case where the asperity fails (Fig. 2b), a decompression on the order of 2 GPa takes place in a few milliseconds or less (solid line, Fig. 2d), so that the process is adiabatic. In the case where the asperity ploughs a permanent furrow into the opposing wall (Fig. 2c) a rapid compression of about the same order (e.g. 2 GPa) occurs (dashed line, Fig. 2d). Therefore, depending on the type of asperity behavior, large adiabatic compressions or decompressions corresponding to the strength of the asperity may take place.

Other mechanisms whereby normal stress rapidly decreases across a slipping fault involve a component of vibration normal to the fault (Melosh, 1996) or separation across the fault due to material property contrasts (Andrews and Ben-Zion, 1997) or stick slip behavior (Brune et al., 1993). These processes, although as yet poorly understood, may also lead to decompression normal to the fault plane.

4. The Joule–Thompson effect

As discussed above, the advance of the asperity over a deformable opposing wall involves either a rapid adiabatic compression or decompression. Depending on the pressure change involved and the properties of the solid, either cooling or heating will occur. The Joule–Thompson coefficient $\mu=(\mathrm{d}T/\mathrm{d}P)_H$ at constant enthalpy H ($=E+PV$, where E in internal energy and PV is pressure–volume work) measures this effect and can be calculated from the expression (Waldbaum, 1971)

$$\mu = V(T\alpha_p - 1)/C_p \tag{3}$$

where V is molar volume (cm^3), T is temperature (K), $\alpha_p=(1/V)(\mathrm{d}V/\mathrm{d}T)$ is the coefficient of volume expansion, and C_p is the isobaric heat capacity (J/cm^3). The Joule–Thompson experiment involved compression of a gas followed by a 'throttled' or muffled adiabatic expansion such that kinetic and potential energies can be neglected; the assumption of gaseous behavior, however, is not required (Adkins, 1983) so that the Joule–Thompson coefficient also applies to solids (Waldbaum, 1971). That the compressions and decompressions are isoenthalpic can be shown as follows. The PV work done w is given by $P_1V_1-P_2V_2$. Since the process is adiabatic, $q=0$ and $\mathrm{d}E=w$. Then $\mathrm{d}E\ (=E_2-E_1)=P_1\mathrm{V}_1-P_2V_2$ and $E_1+P_1V_1=E_2+P_2V_2$, which indicates $H\ (=E+PV)$ is constant (Adkins, 1983). Because the Joule–Thompson coefficient depends on P and T it is an intensive thermodynamic property, and therefore is independent of asperity size.

Table 1 lists values of μ for common silicates at 400 °C based on their physical properties (Skinner, 1966; Robie et al., 1978). All values of μ are negative indicating that cooling occurs on compression and heating on decompression. The μ values do not change substantially over the interval 20–800 °C, except in the case of quartz, where it is close to zero at 800 °C.

The compressive yield strength of the common silicates is listed in Table 1 (Spray, 1992). Experimental rock friction studies indicate these stresses are realized at the asperity tip (Logan and Teufel, 1986; Dietrich and Kilgore, 1996). If compressions and decompressions equivalent to the compressive strength of these minerals occur, then temperature changes in the range ±336–879 °C are possible (Table 1). These temperatures are obtained by multiplying the value of μ by the mineral strength in Table 1. The temperature changes are maximum values insofar as they assume a total stress drop during asperity failure. The temperature changes

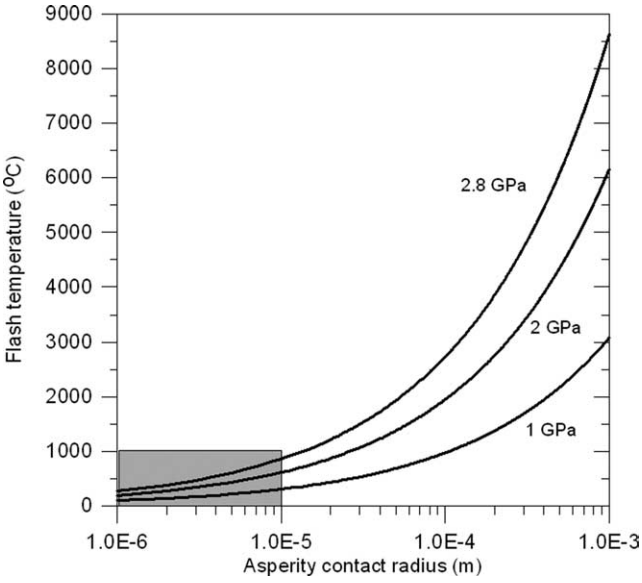

Fig. 3. Flash melt temperatures as a function of asperity contact radius and asperity yield strength, using Eq. (4) in the text (based on Eqs. (11) and (14c) of Archard, 1958–59). Below a 10 μm contact radius, the frictional heating effect is less than 1000 °C for a range of asperity strengths (shaded rectangle).

are in addition to frictional heat developed at the asperity tip, and also in addition to the ambient country rock temperature. If the fault has a fractal roughness, as suggested (Power et al., 1988; Sammis et al., 1999; Scholz, 2002), the process will continue throughout the slip duration over the entire rupture surface.

The heat source on individual asperities will last only a millisecond (for a slip velocity of 1 ms^{-1}), and the distance x over which the temperature change is reduced by diffusion to, say 10% of its original value, is given by $x/2\sqrt{(kt)}=0.08$ (Carslaw and Jaeger, 1985, fig. 5), where t is time and k is the thermal diffusivity ($=3.85\times10^{-6}$ m^2/s for quartz). For times of 1 ms, and 1 s, the heat will have diffused only 10 and 300 μm, respectively. The thermal evolution of individual asperities will be independent of each other on these time and distance scales. Temperature spikes will therefore be highly localized and cannot be averaged over the fault surface.

5. Flash heating temperatures

As pointed out above, the Joule–Thompson coefficient (μ) is independent of asperity size so that the magnitude of the temperature effect is solely the product of asperity strength and μ. However, the frictional heat produced at an asperity tip (the so-called 'flash temperature'; Rabinowicz, 1995) is proportional to the contact area of the asperity, so that as asperity size decreases, the frictional heat generated also decreases. There should exist, therefore, an asperity size below which the Joule–Thompson effect is equal to or greater than the frictional heating effect, and this is addressed below.

Archard (1958–59) provided expressions for estimating the flash temperature in °C to be added to the ambient temperature for a circular asperity sliding on a flat surface which can be recast as:

$$\Delta T = 0.345\,\frac{\mu\pi p_{\mathrm{f}}}{\rho C_{\mathrm{p}}}\sqrt{\frac{rV}{2K}} \tag{4}$$

where μ is coefficient of friction, p_{f} is compressive yield strength, ρ is density, C_{p} is heat capacity at constant pressure, r is asperity contact radius, V is velocity of sliding and $k=(K/\rho C_p)$ is thermal diffusivity, where K is thermal conductivity. In the case of quartz the following values are used: $\mu=0.5$, $p_{\mathrm{f}}=2.8$ GPa (Table 1), $\rho=2650$ kg/m^3, $C_p=$ 756 J/kg/K at 300 K (Robie et al., 1978), $k=3.85\ 10^{-6}$ m^2/s, and $V=1$ ms^{-1}. Fig. 3 shows the flash temperatures for a range of asperity contact radii (1–1000 μm). Because of the smaller sliding area at smaller asperity sizes, the flash temperature decreases with decreasing asperity size. Also shown on Fig. 3 are flash temperatures for lower yield strengths of 1 and 2 GPa. The flash temperatures are less than 1000 °C for an asperity contact radius of 10 μm or less. Since the Joule–Thompson temperature effect for quartz is ±880 °C for a 2.8 GPa pressure change, this effect will be approximately equal to or greater than the frictional heat effect at smaller asperity sizes. These asperity sizes correspond to contact areas of ~300 μm^2, typical of median contact areas in experiments on quartz at different normal stresses (Dieterich and Kilgore, 1996). In the case of Joule–Thompson cooling, the frictional heating effect would be almost entirely cancelled. Conversely, in the case of Joule–Thompson heating, the two effects would be additive.

It is interesting to compare the estimated flash melting temperature of about 1000 °C for asperity contact areas of ~300 μm^2 to estimates of temperatures in natural pseudotachylytes that are typically in the range 750–1450 °C (Toyoshima, 1990; Moecher and Brearley, 2004; Di Toro and Pennacchioni, 2004).

6. Parkfield example

As pointed out above, seismic observations on the San Andreas fault at Parkfield (Nadeau and Johnson, 1998; Sammis et al., 1999) appear to be consistent with experimental observations (Dieterich and Kilgore, 1994, 1996), and suggest that this locality may be used to illustrate the potential role of the Joule–Thompson effect during seismic slip. The seismic and experimental observations together suggest that: (1) a fractal distribution of asperity size versus number exists, involving a spatial clustering of asperities and earthquake epicenters, (2) small earthquakes involved failure of very strong asperities with stress drops on the order of 1–2 GPa, (3) for small earthquakes the

Table 2
Characteristics of asperities for a Cantor dust fractal model

Hierarchy level	# Asperities	Contact radius (m)	Volume[a] (m^3)	Total volume[b] (m^3)	Fault contact area (%)
0	1	0.5	0.2618	0.2618	100
1	10	0.05	0.0002618	0.002618	10
2	100	5×10^{-3}	2.618×10^{-7}	2.62×10^{-5}	1
3	1000	5×10^{-4}	2.618×10^{-10}	2.62×10^{-7}	0.1
4	10,000	5×10^{-5}	2.618×10^{-13}	2.62×10^{-9}	0.01
5	100,000	5×10^{-6}	2.618×10^{-16}	2.62×10^{-11}	0.001

[a] Hemispheres.
[b] Columns 2×4.

largest asperity size was approximately 1 m^2, and (4) the maximum real area of contact was ~0.2%. Sammis et al. (1999) proposed a fractal model for the distribution of asperities at Parkfield: $D=[\log N(r)]/[\log 1/r]$, where D is the fractal dimension, N is the number of asperities, and r is the radius of the asperity. For consistency with moment–displacement relationships at Parkfield, Sammis et al. (1999) choose a 2-D Cantor dust fractal model such that $D=\log 10/\log 10=1$.

Using this fractal model, Table 2 shows several physical characteristics of hemispherical asperities, including asperity number, contact radius, asperity volume and total asperity volume and percentage real contact area, over five hierarchical levels. Fig. 1 shows a plot of asperity stress versus contact area/total fault area for different average fault stresses. For a contact area of 0.1%, and an average fault stress of 1–5 MPa, the asperity stresses range from 500 to 3000 MPa. Sammis et al. (1999) have argued that if some type of healing process inhibits brittle failure, rock asperities can sustain these high stresses. As pointed out above (Fig. 3), for asperity contact radii of 10 μm or less ($<$ 300 μm^2), the Joule–Thompson effect will be equal to or greater than the frictional heating effect at high stress. These asperity contact areas are typical of a variety of materials with normal stress in the range 16–30 MPa (Diterich and Kilgore, 1996). Depending on whether cooling or heating occurs on an asperity, the Joule–Thompson effect may augment or cancel frictional heating, provided the asperities are small enough and strong enough. In order to get a substantial Joule–Thompson effect at Parkfield, it appears from Table 2, that fault contact areas of 0.01–0.001% are required. This conclusion, however, is highly dependent on the geometry of the fractal model.

7. Discussion

A long-standing puzzle is the apparent paucity of pseudotachylytes in the geologic record, despite theoretical studies that suggest they should be common (Sibson, 1975; Cardwell et al., 1978). The large literature on pseudotachylytes suggests their lack of recognition in the field is not due to unfamiliarity with this rock type. Other explanations for their rarity are that frictional heat may be generated over a wider fault zone width than assumed, resulting in lower temperatures. Thermal pressurization, without melting, may also reduce effective stress resulting in less frictional heat generated (Mase and Smith, 1984; Noda, 2004). At high slip velocities, friction coefficients may also be lower than commonly assumed (Mizoguchi and Shimamoto, 2004; Di Toro et al., 2004), so that less heat is generated. At present, it is unclear which, if any, of these explanations is correct. An additional factor, suggested by this study, is that adiabatic compression beneath an asperity may cause substantial cooling, thereby canceling the frictional heat generated at the asperity tip. As pointed out above, asperity temperature spikes are highly localized so that heating and cooling effects cannot be averaged over the fault surface. Lineations are common features of fault surfaces (e.g. slickensides) that may represent abrasive wear whereby a strong asperity ploughs a groove in the opposing wall. If this type of abrasive wear is common during seismic slip (Fig. 2c), then cooling due to adiabatic compression may be as important as heating.

Acknowledgements

I thank S. Karner and anonymous reviewers for helpful comments on earlier versions of the manuscript and the editorial help of D. Ferrill. An anonymous reviewer kindly recast Archard's equations into the more tractable form used here. Partly supported by NSF-EAR-0003482.

References

Adkins, C.J., 1983. Equilibrium Thermodynamics, 3rd ed Cambridge Press, New York.

Andrews, D.J., Ben-Zion, Y., 1997. Wrinkle-like slip pulse on a fault between different materials. J. Geophys. Res. 102, 553–571.

Archard, J.F., 1958/. The temperature of rubbing surfaces. Wear 2, 438–455.

Bjornerud, M., Magloughlin, J.F., 2004. Pressure-related feedback processes in the generation of pseudotachylytes. J. Struct. Geol. 26, 2317–2323.

Brune, J.N., Brown, S., Johnson, P.A., 1993. Rupture mechanism and interface in foam rubber models of earthquakes: a possible solution to the heat flow paradox and the paradox of large overthrusts. Tectonophysics 218, 59–67.

Cardwell, P.K., Chinn, D.S., Moore, G.F., Turcotte, D.L., 1978. Frictional heating on a fault zone with finite thickness. Geophys. J.R. Astron. Soc. 52, 525–530.

Carslaw, H.S., Jaeger, J.C., 1985. Conduction of Heat in Solids, 2nd ed. 1985, Oxford, 510pp.

Dieterich, J.H., Kilgore, B.D., 1994. Direct observation of frictional contacts: new insights for state-dependant properties. Pure Appl. Geophys. 143, 283–301.

Dieterich, J.H., Kilgore, B.D., 1996. Imaging surface contacts: power law contact distributions and contact stresses in quartz, calcite, glass and acrylic plastic. Tectonophysics 256, 219–239.

Di Toro, G., Pennacchioni, G., 2004. Superheated friction-induced melts in zoned pseudotachylytes within the Adamello tonalities (Italian Southern Alps). J. Struct. Geol. 26, 1783–1801.

Di Toro, G., Goldsby, D.L., Tullis, T.E., 2004. Friction falls toward zero in quartz rock as slip velocity approaches seismic rates. Nature 427, 436–438.

Jaeger, J.C., Cook, N.G.W., 1979. Fundamentals of Rock Mechanics, 2nd ed. Chapman & Hall, London.

Logan, J.M., Teufel, L.W., 1986. The effect of normal stress on the real area of contact during frictional sliding in rocks. Pure Appl. Geophys. 124, 471–486.

Mase, C.W., Smith, L., 1984. Pore-fluid pressure and frictional heating on a fault plane. Pure Appl. Geophys. 122, 583–607.

Melosh, H.J., 1989. Impact Cratering: A Geologic Process, Oxford Monographs on Geology and Geophysics No. 11. Oxford University Press.

Melosh, H.J., 1996. Dynamical weakening of faults by acoustic fluidization. Nature 379, 601–606.

Mizoguchi, K., Shimamoto, T., 2004. Dramatic slip weakening of Nojima fault gouge at high velocities and its implication for dynamic fault motion. AGU San Francisco meeting, December 13–17, T23A-0559.

Moecher, D.P., Brearley, A.J., 2004. Mineralogy and petrology of a mullite-bearing pseudotachylyte: constraints on the temperature of coseismic frictional fusion. Am. Mineral. 89, 1485–1496.

Nadeau, R.M., Johnson, L.R., 1998. Seismological studies at Parkfield VI: moment release rates and estimates of source parameters for small repeating earthquakes. Bull. Seismol. Soc. Am. 88, 790–814.

Noda, H., 2004. Numerical simulation of rupture propagation with thermal pressurization based on measured hydraulic properties: the importance of deformation zone width. AGU Fall Meeting, San Francisco, December 13–17, T22A-08.

O'Hara, K., 2001. A pseudotachylyte geothermometer. J. Struct. Geol. 23, 1345–1357.

Power, W.L., Tullis, T.E., Weeks, J.D., 1988. Roughness and wear during brittle faulting. J. Geophys. Res. 93, 15268–15278.

Rabinowicz, E., 1995. Friction and Wear of Materials, 2nd ed. Wiley, New York. 314pp.

Robie, R.A., Hemingway, B.S., Fisher, J.R., 1978. Thermodynamic properties of minerals and related substances at 298.15 K and 1 bar pressure and at higher temperatures. US Geol. Surv. Bull., 1452.

Sammis, C.G., Nadeau, R.M., Johnson, L.R., 1999. How strong is an asperity? J. Geophys. Res. B104 (10), 609–610.

Scholz, C.H., 1987. Wear and gouge formation in brittle faulting. Geology 15, 493–495.

Scholz, C.H., 2002. The Mechanics of Earthquakes and Faulting, 2nd ed Cambridge Press, New York. 470pp.

Sibson, R.H., 1975. Generation of pseudotachylyte by ancient seismic faulting. Geophys. J. R. Astron. Soc. 43, 775–794.

Skinner, B.J., 1966. Thermal expansion. In: Clark, S.P. (Ed.), Handbook of Physical Constants Geological Society of America Memoir, vol. 97, pp. 75–96.

Spray, J., 1992. A physical basis for the frictional melting of some rock-forming minerals. Tectonophysics 204, 205–221.

Spray, J., 1995. Pseudotachylyte controversy, fact or friction. Geology 23, 1119–1122.

Toyoshima, T., 1990. Pseudotachylite from the Main zone of the Hidaka metamorphic belt, Hokaido, northern Japan. J. Met. Geol. 8, 505–523.

Waldbaum, D.R., 1971. Temperature changes associated with adiabatic decompression in Geological processes. Nature 232, 545–548.